ATLAS Draft

Measurement of the $t\bar{t}$ production cross section in the tau + jets channel using the ATLAS detector

Version: 2.0

To be submitted to: EPJC

Corresponding editor(s)

Pier-Olivier DeViveiros (viveiros@nikhef.nl)
Olga Igonkina (Olga.Igonkina@cern.ch)
Joerg Mechnich (Joerg.Mechnich@nikhef.nl)

A list of supporting internal notes and their authors can be found at:

ATL-COM-PHYS-2011-1532 https://cdsweb.cern.ch/record/1409744

Comments are due by: October 4th

document created on October 22, 2012 from file main.tex
cover page automatically created with atlascover.sty

Eur. Phys. J. C manuscript No.
(will be inserted by the editor)

Measurement of the $t\bar{t}$ production cross section in the tau+jets channel using the ATLAS detector

The ATLAS Collaboration

[1]CERN, 1211 Geneva 23, Switzerland

October 22, 2012

Abstract In this document, a measurement of the top quark pair production cross section in the final state with a hadronically decaying tau lepton and jets is presented. The analysis is based on proton-proton collision data recorded by the ATLAS experiment at the LHC, with a centre-of-mass energy of 7 TeV. The data sample used corresponds to an integrated luminosity of 1.67 fb^{-1}. The cross section is measured to be $\sigma_{t\bar{t}} = 194 \pm 18$ (stat.) $\pm$ 46 (syst.) pb and is in agreement with other measurements and with the Standard Model prediction.

1 Introduction

At the Large Hadron Collider (LHC), top quark pairs ($t\bar{t}$) are produced in abundance due to the high centre-of-mass energy of 7 TeV. The large sample of $t\bar{t}$ events collected with the ATLAS detector, corresponding to an integrated luminosity of 1.67 fb^{-1}, makes it possible to study experimentally challenging decay channels and topologies. This paper describes a measurement of the $t\bar{t}$ production cross section. The studied final state consists of a hadronically decaying tau lepton (τ_{had}) and jets, corresponding to the $t\bar{t} \to [b\tau_{\text{had}}\nu_\tau][bqq]$ decay, where b and q are used to denote b-quarks and lighter quarks, respectively. Such an event topology with a hadronically decaying tau lepton corresponds to approximately 10% of all $t\bar{t}$ decays [1].

A $t\bar{t}$ cross section measurement in the final state with tau leptons makes it possible to probe flavour-dependent effects in top quark decays. It is also relevant in the scope of searches for processes beyond the Standard Model, where $t\bar{t}$ events with tau leptons in the final state are a dominant background. This is particularly important for an hypothetical charged Higgs boson production [2–5] in top quark decays, where the existence of a charged Higgs boson would lead to an enhancement in the cross section for the considered $t\bar{t}$ final state which cannot be seen in other channels. The measurement presented here is complementary to the previously published tau + lepton channel measurement [6]. The most recent cross section measurements of the tau + jets decay channel have been performed by the CDF and D0 experiments in proton-antiproton collisions at $\sqrt{s} = 1.96$ TeV [7, 8]. This is the first measurement conducted in this specific channel at the LHC.

In this analysis, events with at least five jets are selected, where two of the jets are identified as having originated from b-quarks. One of the remaining jets is selected as the τ_{had} candidate based on the reconstruction of the top quark decays. The τ_{had} contribution is separated from quark- or gluon-initiated jets with a one-dimensional fit to the number of tracks associated with the τ_{had} candidate. Since the τ_{had} decays preferentially to one or three charged particles (and other neutral decay products), this variable offers a good separation between hadronically-decaying tau leptons and jets, as the latter typically produce a large number of charged particles. The main backgrounds to the $t\bar{t}$ signal come from multijet events, $t\bar{t}$ events with a different final state or signal events where the wrong jet is chosen as the τ_{had} candidate. A small contribution from single top and W+jets events is also present. The distributions for the backgrounds used in the fit are obtained with data-driven methods.

2 The ATLAS Detector

The ATLAS detector [9] is a multipurpose particle physics detector with an approximately forward-backward symmetric cylindrical geometry and a near-4π coverage in solid angle[1]. The inner tracking detector covers the pseudorapidity range $|\eta| < 2.5$, and consists of a silicon pixel detector, a silicon microstrip detector (SCT), and, for $|\eta| < 2.0$, a transition radiation tracker. The inner detector is surrounded by a thin superconducting solenoid providing a 2 T magnetic field along the beam direction. A high-granularity liquid-argon sampling electromagnetic calorimeter covers the region $|\eta| < 3.2$. An iron-scintillator tile hadronic calorimeter provides coverage in the range $|\eta| < 1.7$. The end-cap and forward regions, spanning $1.5 < |\eta| < 4.9$, are instrumented with liquid-argon calorimeters for both electromagnetic and hadronic measurements. The muon spectrometer surrounds the calorimeters. It consists of three large air-core superconducting toroid systems and separate trigger and high-precision tracking chambers providing accurate muon tracking for $|\eta| < 2.7$.

3 Data and Simulation Samples

The data used in this analysis were collected during the first half of the 2011 data taking period and correspond to a total integrated luminosity of $\mathcal{L} = 1.67$ fb^{-1}. The data sample was selected with a b-jet trigger that requires at least four jets identified with $|\eta| < 3.2$ and a transverse energy (E_{T}) above 10 GeV. Two of these jets are required to be identified as b-jets using a dedicated high-level-trigger b-tagging algorithm [10].

The selection efficiency for the $t\bar{t} \to \tau_{had}$ + jets signal is derived from Monte Carlo (MC) simulations. The `MC@NLO` v4.01 [11] generator, with the parton distribution function (PDF) set `CT10` [12], is used for the $t\bar{t}$ signal. The theoretical prediction of the $t\bar{t}$ cross section for proton-proton collisions at a centre-of-mass energy of $\sqrt{s} = 7$ TeV is $\sigma_{t\bar{t}} = 167^{+17}_{-18}$ pb for a top quark mass of 172.5 GeV. It has been calculated at approximate next-to-next-to-leading order (NNLO) in QCD with `Hathor 1.2` [13] using the `MSTW2008` 90% CL NNLO PDF sets [14], incorporating PDF+α_S uncertainties according to the `MSTW` prescription [15] and cross checked with the `NLO+NNLL` calculation of Cacciari et al. [16] as implemented in `Top++` 1.0 [17]. Tau lepton decays are modeled with `TAUOLA` [18]. Samples of simulated events are also used to estimate the small contributions from W+jets, Z+jets, single top and diboson events, as described in [19]. The generated events were processed through the full ATLAS detector simulation using `GEANT4` [20, 21], followed by the trigger and offline reconstruction. The distribution of the number of pile-up events (i.e. collisions in the same bunch crossing as the hard-scattering event) was adjusted to match the occupancies measured in the data.

4 Event Selection

Jets are reconstructed from clusters of calorimeter cells [22] using the anti-k_t algorithm [23, 24] with a distance parameter $R = 0.4$. The jets are calibrated using transverse momentum- and η-dependent corrections obtained from simulation and validated with collision data [25]. Candidate events are required to contain at least five jets with a transverse momentum (p_{T}) larger than 20 GeV and $|\eta| < 2.5$.

The identification of jets originating from b-quarks is performed using algorithms that combine secondary vertex properties and track impact parameters [26]. The algorithm identifies b-jets with an average efficiency of 60% and provides a light-quark jet rejection factor of about 340 in $t\bar{t}$ topologies. The likelihood of misidentifying a τ_{had} as a b-jet in a $t\bar{t}$ event is approximately 5%. The two b-jets with the highest b-tag probability are chosen as the event b-candidates; events with less than two b-jets are rejected.

The missing transverse momentum ($E_{\mathrm{T}}^{\mathrm{miss}}$) is reconstructed from energy clusters in the calorimeters. The calibration of each cluster is dependent on the type of physical object associated with the cluster. The transverse momenta of muons in the event are also taken into account. The $E_{\mathrm{T}}^{\mathrm{miss}}$ significance ($S_{E_{\mathrm{T}}^{\mathrm{miss}}}$) is defined as $E_{\mathrm{T}}^{\mathrm{miss}}/(0.5\ [\sqrt{\mathrm{GeV}}] \cdot \sqrt{\Sigma E_{\mathrm{T}}})$, where ΣE_{T} is the scalar sum of the transverse momenta of all objects. Using a $S_{E_{\mathrm{T}}^{\mathrm{miss}}}$ requirement instead of a direct $E_{\mathrm{T}}^{\mathrm{miss}}$ requirement allows the rejection of multijet events where the $E_{\mathrm{T}}^{\mathrm{miss}}$ arises from energy resolution effects, while still retaining high efficiency for signal events with $E_{\mathrm{T}}^{\mathrm{miss}}$ coming from particles which do not interact with the detector [27]. Candidate events are required to have $S_{E_{\mathrm{T}}^{\mathrm{miss}}} > 8$.

To reduce the background due to events containing W bosons that decay leptonically and to avoid overlap with other $t\bar{t}$ cross section measurements, events containing a reconstructed electron or muon [28, 29] with $p_{\mathrm{T}} > 15$ GeV and $|\eta| < 2.5$ are vetoed.

[1] ATLAS uses a right-handed coordinate system with its origin at the nominal interaction point (IP) in the centre of the detector and the z-axis along the beam pipe. The x-axis points from the IP to the centre of the LHC ring, and the y axis points upward. Cylindrical coordinates (r, ϕ) are used in the transverse plane, ϕ being the azimuthal angle around the beam pipe. The pseudorapidity is defined in terms of the polar angle θ as $\eta = -\ln\tan(\theta/2)$. The variable ΔR is used to evaluate the distance between objects, and is defined as $\Delta R = \sqrt{(\Delta\phi)^2 + (\Delta\eta)^2}$.

In each event, a single $\tau_{\rm had}$ candidate is selected from the reconstructed jets using the following procedure. First, the reconstruction of the hadronically decaying top-quark is attempted by selecting the three jets (including exactly one of the two b-candidates) that give the highest four-vector $p_{\rm T}$ sum. The remaining jet with the highest $p_{\rm T}$, excluding the remaining b-candidate, is selected as the $\tau_{\rm had}$ candidate. Events where the $\tau_{\rm had}$ candidate $p_{\rm T}$ is below 40 GeV are rejected.

The main contributions to the selected $\tau_{\rm had}$ candidates in the signal region come from the signal ($\tau_{\rm had}$ from $t\bar{t}$ events), electrons from $t\bar{t}$ events and misidentified jets from $t\bar{t}$, single top, W + jets and multijet events. The contributions from $Z/\gamma^{\star}$ + jets and diboson processes are negligible.

5 Data Analysis

The majority of $\tau_{\rm had}$ decays are characterised by the presence of one or three charged hadrons in the final state, which can be reconstructed as charged particle tracks in the inner detector. The number of tracks ($n_{\rm track}$) originating from the interaction point is used to separate $\tau_{\rm had}$ from the misidentified jet backgrounds.

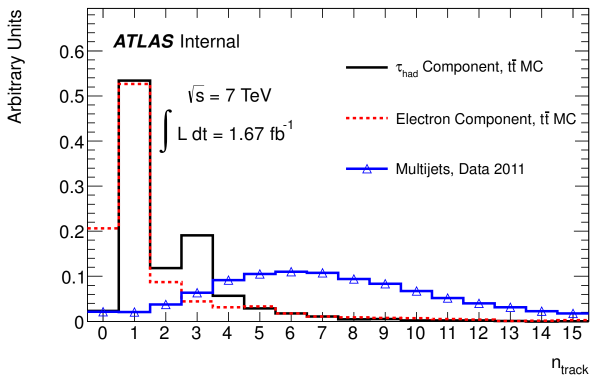

Fig. 1 Distribution of $n_{\rm track}$ for $\tau_{\rm had}$ from MC $t\bar{t}$ events (solid black line), electrons from MC $t\bar{t}$ events (dashed red line), and for jets from multijet events from data (blue triangles). The multijet event selection uses a $S_{E_{\rm T}^{\rm miss}}$ sideband region as described in Section 5. All distributions are normalised to unity.

All selected tracks with $p_{\rm T}$ > 1 GeV located in a core region of size ΔR < 0.2 around the jet axis are counted. To increase the discriminating power, tracks in the outer cone 0.2 < ΔR < 0.6 are also counted, using a variable $p_{\rm T}$ requirement that is dependent on both the ΔR of the outer track and the $p_{\rm T}$ of the core tracks. This variable $p_{\rm T}$ requirement was designed to reduce the contribution from pile-up and underlying event tracks, and is explained in [30]. The separation power of the $n_{\rm track}$ variable is illustrated in Fig. 1 where a comparison of the $n_{\rm track}$ distribution is shown for $\tau_{\rm had}$, electrons and misidentified jets from multijet events.

To extract the signal from the $n_{\rm track}$ distribution, the data sample is fitted with three probability distribution functions (templates): a *tau/electron* template, a *gluon-jet* template and a *quark-jet* template. The $\tau_{\rm had}$ component from $t\bar{t}$ events constitutes the signal in the event sample. Real electrons (either prompt or from leptonic tau decays) from $t\bar{t}$ events which failed to be rejected by the veto also contribute significantly to the event sample. The electron and $\tau_{\rm had}$ templates are combined into a single *tau/electron* template to ensure a stable fit. The *tau/electron* template is obtained from simulated $t\bar{t}$ events. The small expected contributions to the real *tau/electron* component of the fit from single top and W + jets events do not change the shape of the template.

The remaining significant contributions come from misidentified jets, and are separated into two templates. The *gluon-jet* template describes the multijet processes which are dominated by gluon-initiated jets, and the *quark-jet* template describes the remaining processes ($t\bar{t}$, single top and W + jets) that are enriched in quark-initiated jets.

The *gluon-jet* template is determined using a sideband region where the $S_{E_{\rm T}^{\rm miss}}$ requirement is relaxed to $3 < S_{E_{\rm T}^{\rm miss}} < 4$. This selections greatly enhances the contribution from multijet events, reducing other contributions (e.g. from $t\bar{t}$ events) to less than 1%. The regions defined by the selection $2 < S_{E_{\rm T}^{\rm miss}} < 3$ and $4 < S_{E_{\rm T}^{\rm miss}} < 5$ are also used to study any correlations between the $S_{E_{\rm T}^{\rm miss}}$ criteria and the $n_{\rm track}$ distribution.

The *quark-jet* template is obtained from a $t\bar{t}$ control sample where the $\tau_{\rm had}$ candidate is replaced by a muon candidate. The reconstructed muon [29] is required to have $p_{\rm T}$ > 20 GeV, $|\eta|$ < 2.5 and no jet within ΔR < 0.4. The requirement on the number of non-b-tagged jets is changed from three to two as the jet corresponding to the $\tau_{\rm had}$ is now replaced by a muon. The other selection requirements are the same as for the signal region. This isolates $t\bar{t}$ events with very high purity: the contribution from backgrounds is at the 5% level, mainly from single top and W + jets events. The two highest $p_{\rm T}$ jets that are not identified as b-jet candidates are selected as $\tau_{\rm had}$ candidates. The template is corrected using MC simulations for differences in the transverse momentum distribution between the signal region and the control sample, and for the expected contribution to the control sample from $t\bar{t}$ dilepton events ($t\bar{t} \rightarrow \mu + \tau_{\rm had} + X$, $t\bar{t} \rightarrow \mu + e + X$).

6 Results

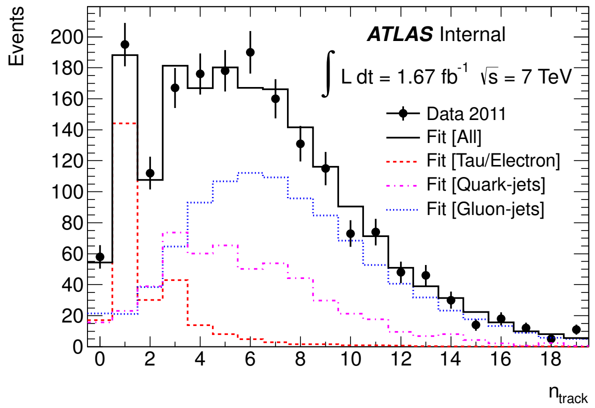

Fig. 2 The n_{track} distribution for τ_{had} candidates after all selection cuts. The black points correspond to data, while the solid black line is the result of the fit. The red (dashed), blue (dotted) and magenta (dash-dotted) histograms show the fitted contributions from the *tau/electron* signal, and the *gluon-jet* and *quark-jet* backgrounds, respectively.

Source	Number of events
tau/electron	
$t\bar{t}$ (τ_{had})	170 ± 40
$t\bar{t}$ (electrons)	47 ± 11
Single top	12 ± 2
W + jets	9 ± 5
Total expected	240 ± 50
Fit result	270 ± 24 (stat.) ± 11 (syst.)
quark-jet	
$t\bar{t}$ (jets)	540 ± 160
Single top	24 ± 4
W + jets	21 ± 12
Total expected	580 ± 160
Fit result	520 ± 97 (stat.) ± 78 (syst.)
gluon-jet	
Fit result	960 ± 77 (stat.) ± 74 (syst.)

Table 1 Comparison of the numbers of events from MC expectations and from the results of the fit to the data for the three templates. The uncertainties on the MC expectations include the systematic uncertainties of the selection efficiency described in Section 7. No MC predictions are available for the *gluon-jet* contribution.

An extended binned-likelihood fit is used to extract the different contributions from the n_{track} distribution. To improve the fit stability, the ratio of the number of *quark-jet* events to *tau/electron* events is constrained with a Gaussian uncertainty. Both contributions are dominated by events from the same process ($t\bar{t}$ events), and their relative production rate is consequently well understood. The width of the Gaussian is determined to be 19% of its central value based on studies of the associated systematic uncertainties. The statistical uncertainties on the fit parameters are calculated using the shape of the fit likelihood. The systematic uncertainties on the shapes of the templates are propagated using a pseudo-experiment approach, taking into account the bin-by-bin correlations. This yields a final number of *tau/electron* events of 270 ± 24 (stat.) ± 11 (syst.).

The fit results are shown in Fig. 2. A comparison between the fit results, and the expected event yields from the MC predictions is presented in Tab. 1. The numbers are in good agreement.

To extract the number of signal events, predictions from simulation are used to subtract the backgrounds from W + jets and single top events (9 ± 5 and 12 ± 2, respectively) from the fitted number of *tau/electron* events. The number is then scaled by the expected ratio of τ_{had} and electrons passing the selection in the $t\bar{t}$ sample. This ratio, $N_\tau/(N_\tau + N_e)$, is estimated from MC simulation to be 0.78 ± 0.03 (stat.) ± 0.03 (syst.). This yields a final number of observed signal events of: $N_\tau = 194 \pm 18$ (stat.) ± 11 (syst.).

The cross section is obtained using $\sigma_{t\bar{t}} = N_\tau/(\mathcal{L} \cdot \varepsilon)$. The efficiency ($\varepsilon$) is estimated from MC simulation to be $(6.0 \pm 1.4) \times 10^{-4}$. It includes the branching fractions for the different $t\bar{t}$ decays and the acceptance. The efficiency is corrected for a 13% difference between MC simulation and data in the trigger and b-tagging efficiencies [26]. The method used for obtaining the uncertainty on the cross section is detailed in Section 7.

The cross section is measured to be $\sigma_{t\bar{t}} = 194 \pm 18$ (stat.) ± 46 (syst.) pb.

7 Systematic Uncertainties

A summary of all systematic uncertainties on the cross section is given in Table 2.

The uncertainty on the selection efficiency due to the choice of MC simulation configuration is estimated by using alternative MC samples and reweighting procedures. The difference in the efficiency obtained from different configurations is taken as the uncertainty. The full details of the samples, generators and procedures used for this study are documented in detail in Ref. [19]. Uncertainties are evaluated on the initial- and final-state radiation (ISR/FSR), hadronisation and pile-up modeling, choice of MC event generator and PDFs.

Uncertainties on the simulation of the detector response are taken into account using dedicated studies of the reconstructed physics objects (electrons, muons, jets, $E_{\text{T}}^{\text{miss}}$). The considered uncertainties are associ-

Source of uncertainty	Relative uncertainty
ISR/FSR	15%
Event generator	11%
Hadronisation model	6%
PDFs	2%
Pile-up	1%
b-jet tagging efficiency	9%
Jet energy scale	5%
$E_{\mathrm{T}}^{\mathrm{miss}}$ significance mismodeling	5%
b-jet trigger efficiency	3%
Jet energy resolution	2%
Fit systematic uncertainties	4%
Luminosity	4%
Total uncertainty	24%

Table 2 Systematic uncertainties on the $t\bar{t}$ cross section.

ated with the jet energy scale, jet energy resolution, b-tagging efficiency, trigger efficiency and $E_{\mathrm{T}}^{\mathrm{miss}}$ calculation. The uncertainty due to a mismodeling of the lepton veto is estimated using the uncertainties on the muon and electron reconstruction efficiencies determined from independent data samples, and is found to be negligible.

To obtain the uncertainty on the fit results, variations are applied to the templates to describe various systematic effects. As the *tau/electron* template is taken directly from MC-simulated $t\bar{t}$ events, the systematics on this template are taken from estimates of the mismodeling of the simulation. The dominant contributions come from variations in the amount of ISR/FSR in the simulation (1%) [31], the modeling of the pile-up (1%), and the statistical uncertainties (1%). Uncertainties on the track reconstruction efficiency, jet energy scale, and ratio of τ_{had} to electrons were found to be negligible. The *quark-jet* template is obtained from a $t\bar{t}$ μ + jets control sample in data. The dominant contributions come from the statistical uncertainties (4%), the difference in shape between the μ + jets template and the expected *quark-jet* distribution, estimated from MC samples (2%), and the MC-based subtraction of the dilepton contribution (1%). The uncertainty on the MC-based kinematic correction is found to be negligible. The *gluon-jet* template is derived from a background-dominated sideband region with low values of $S_{E_{\mathrm{T}}^{\mathrm{miss}}}$. The two sources of uncertainties are the dependence of the template on the $S_{E_{\mathrm{T}}^{\mathrm{miss}}}$ criteria of the control region, obtained by varying the $S_{E_{\mathrm{T}}^{\mathrm{miss}}}$ requirements (1%), and the statistical uncertainty of the control region (1%). The total systematic uncertainty on the fit is found to be 4%.

The uncertainty on the luminosity is calculated to be 4% as described in Ref. [32]. The total uncertainty on the cross section is 24%.

8 Conclusions

This document presents a measurement of the top quark pair production cross section in the final state corresponding to the $t\bar{t} \to [b\tau_{\mathrm{had}}\nu_\tau][bqq]$ decay. The measurement uses a dataset corresponding to an integrated luminosity of 1.67 fb^{-1} of proton-proton collision data at a centre-of-mass energy of 7 TeV recorded by the ATLAS experiment at the LHC. The signal was extracted by fitting the number of tracks associated to the tau lepton candidate with templates derived from simulation for the $t\bar{t}$ signal and from the data for the backgrounds.

The $t\bar{t}$ production cross section is measured to be $\sigma_{t\bar{t}} = 194 \pm 18$ (stat.) $\pm$ 46 (syst.) pb. The result presented here is in agreement with the theoretical prediction of 167^{+17}_{-18} pb, as well as the latest combination of different ATLAS analyses yielding 177 $\pm$ 3 (stat.) $^{+8}_{-7}$ (syst.) $\pm$ 7 (lumi.) pb [33].

9 Acknowledgements

We thank CERN for the very successful operation of the LHC, as well as the support staff from our institutions without whom ATLAS could not be operated efficiently.

We acknowledge the support of ANPCyT, Argentina; YerPhI, Armenia; ARC, Australia; BMWF, Austria; ANAS, Azerbaijan; SSTC, Belarus; CNPq and FAPESP, Brazil; NSERC, NRC and CFI, Canada; CERN; CONICYT, Chile; CAS, MOST and NSFC, China; COLCIENCIAS, Colombia; MSMT CR, MPO CR and VSC CR, Czech Republic; DNRF, DNSRC and Lundbeck Foundation, Denmark; EPLANET and ERC, European Union; IN2P3-CNRS, CEA-DSM/IRFU, France; GNAS, Georgia; BMBF, DFG, HGF, MPG and AvH Foundation, Germany; GSRT, Greece; ISF, MINERVA, GIF, DIP and Benoziyo Center, Israel; INFN, Italy; MEXT and JSPS, Japan; CNRST, Morocco; FOM and NWO, Netherlands; RCN, Norway; MNiSW, Poland; GRICES and FCT, Portugal; MERYS (MECTS), Romania; MES of Russia and ROSATOM, Russian Federation; JINR; MSTD, Serbia; MSSR, Slovakia; ARRS and MVZT, Slovenia; DST/NRF, South Africa; MICINN, Spain; SRC and Wallenberg Foundation, Sweden; SER, SNSF and Cantons of Bern and Geneva, Switzerland; NSC, Taiwan; TAEK, Turkey; STFC, the Royal Society and Leverhulme Trust, United Kingdom; DOE and NSF, United States of America.

The crucial computing support from all WLCG partners is acknowledged gratefully, in particular from CERN and the ATLAS Tier-1 facilities at TRIUMF (Canada), NDGF (Denmark, Norway, Sweden), CC-IN2P3 (France), KIT/GridKA (Germany), INFN-CNAF (Italy), NL-T1 (Netherlands), PIC (Spain), ASGC (Taiwan), RAL (UK) and BNL (USA) and in the Tier-2 facilities worldwide.

References

1. J. Beringer et al. (Particle Data Group), Phys. Rev. **D86**, 010001 (2012)
2. J.F. Gunion, H.E. Haber, G. Kane, S. Dawson, *The Higgs Hunter's Guide* (Addison-Wesley, 1990)
3. J.F. Gunion, H.E. Haber, G. Kane, S. Dawson, Errata for "The Higgs Hunter's Guide". preprint SCIPP-92-58 (1993)
4. J.F. Gunion, H.E. Haber, Nucl. Phys. **B272**, 1 (1986)
5. ATLAS Collaboration, JHEP **1206**, 039 (2012)
6. ATLAS Collaboration, Accepted by Phys. Lett. B, arXiv:1205.2067 [hep-ex] (2012)
7. V. M. Abazov et al. (D0 Collaboration), Phys. Rev. **D82**, 071102 (2010)
8. T. Aaltonen et al. (CDF Collaboration), Accepted by Phys. Rev. Lett., arXiv:1208.5720 [hep-ex] (2012)
9. ATLAS Collaboration, JINST **3**, S08003 (2008)
10. ATLAS Collaboration, Eur. Phys. J. **C72**, 1849 (2012)
11. S. Frixione, B.R. Webber, JHEP **06**, 029 (2002)
12. H.L. Lai, et al., Phys. Rev. **D82**, 074024 (2010)
13. M. Aliev, H. Lacker, U. Langenfeld, S. Moch, P. Uwer, M. Wiedermann, Comput. Phys. Commun. **182**, 1034 (2011)
14. A. Martin, W. Stirling, R. Thorne, G. Watt, Eur. Phys. J. **C63**, 189 (2009)
15. A. Martin, W. Stirling, R. Thorne, G. Watt, Eur. Phys. J. **C64**, 653 (2009)
16. M. Cacciari, M. Czakon, M.L. Mangano, A. Mitov, P. Nason, arXiv: hep-ph/1111.5869
17. M. Czakon, A. Mitov, arXiv: hep-ph/1112.5675
18. S. Jadach, Z. Wąs, R. Decker, J.H. Kühn, Comput. Phys. Commun. **76**, 361 (1993)
19. ATLAS Collaboration, Eur. Phys. J. **C71**, 1577 (2011)
20. S. Agostinelli, et al., Nucl. Instrum. Meth. **A506**, 250 (2003)
21. ATLAS Collaboration, Eur. Phys. J. **C70**, 823 (2010)
22. ATLAS Collaboration. Calorimeter clustering algorithms: Description and performance. ATL-LARG-PUB-2008-002, http://cdsweb.cern.ch/record/1099735
23. M. Cacciari, G.P. Salam, Phys. Lett. **B641**, 57 (2006)
24. M. Cacciari, G.P. Salam, G. Soyez, JHEP **0804**, 063 (2008)
25. ATLAS Collaboration, submitted to Eur. Phys. J., arXiv:1112.6426[hep-ex]
26. ATLAS Collaboration. Commissioning of the ATLAS high-performance b-tagging algorithms in the 7 TeV collision data. ATLAS-CONF-2011-102, http://cdsweb.cern.ch/record/1369219
27. ATLAS Collaboration, Phys. Lett. **B706**, 276 (2012)
28. ATLAS Collaboration, Eur. Phys. J. **C72**, 1909 (2012)
29. ATLAS Collaboration. Muon reconstruction efficiency in reprocessed 2010 LHC proton-proton collision data recorded with the ATLAS detector. ATLAS-CONF-2011-063, http://cdsweb.cern.ch/record/1345743
30. ATLAS Collaboration. Performance of the Reconstruction and Identification of Hadronic Tau Decays in ATLAS with 2011 Data. ATLAS-COM-CONF-2012-080, http://cdsweb.cern.ch/record/1450096
31. ATLAS Collaboration. Expected Performance of the ATLAS Experiment — Detector, Trigger and Physics. CERN-OPEN-2008-020, https://cdsweb.cern.ch/record/1125884
32. ATLAS Collaboration. Luminosity Determination in pp Collisions at $\sqrt{s} = 7$ TeV using the ATLAS Detector in 2011. ATLAS-CONF-2011-116, http://cdsweb.cern.ch/record/1376384
33. ATLAS Collaboration. Statistical combination of top quark pair production cross-section measurements using dilepton, single-lepton, and all-hadronic final states at $\sqrt{s} = 7$ TeV with the ATLAS detector. ATLAS-CONF-2012-024, http://cdsweb.cern.ch/record/1430733